

# Boundary Conditions and Particle Loading for the Modeling of a Semi-infinite Plasma

G. Gozadinos, D. Vender, and M. M. Turner

*Plasma Research Laboratory, School of Physical Sciences and National Center for Plasma Science and Technology, Dublin City University, Dublin 9, Ireland*

E-mail: gg@physics.dcu.ie

Received December 13, 2000; revised April 26, 2001

---

We present a method for the treatment of the boundary conditions and the particle loading in a self-consistent semi-infinite Particle-In-Cell simulation. We assume a nonionizing, collisional plasma in contact with an electrode. The simulation is planar and one-dimensional (1d-2v), and is driven by an *rf* and/or DC current source. The particle loading is done by appropriate drifting velocity distributions, both for ions and electrons. Limiting the simulation to the region immediately adjacent to the electrode dramatically improves run-times and diagnostic resolution and is ideal for studying the sheath and plasma-sheath interface independently from the rest of the plasma. The method can be generalized easily to model cylindrical and spherical geometries, and surface processes can also be included. The control parameters of the simulation are the values for the current drive ( $I_{rf}$ ,  $\omega_{rf}$ ,  $I_{DC}$ ), the species temperatures in the bulk plasma  $T_s$ , and the values of the ion fluxes  $\Gamma_s$ . © 2001 Academic Press

*Key Words:* PIC simulation; sheath; presheath; Langmuir probes; semi-infinite plasma; boundary layer.

---

## 1. INTRODUCTION

It is often desirable to model plasma dynamics in the vicinity of an electrode, independently of the bulk of the plasma. This is of particular importance when attempting to model sheath dynamics or the plasma-sheath transition through a presheath. Analytical [1–3] or semi-analytical [4] models dealing with these problems are desirable, but at the same time are bound to be subject to problems having to do with the assumptions used or a lack of self-consistency. In addition, the natural presence of two separate spatial scales in this problem (the sheath scale being the electron Debye length  $\lambda_D$ , whereas the bulk plasma/presheath scale being the ion mean free path  $L$ ) requires special treatment of the boundary layer and poses difficulties to analytical approaches (see discussion in [5]).

In such cases, the Particle-In-Cell [6–10] scheme presents an interesting alternative. The drawback, however, is that the nature of the problem requires that the boundary on the bulk-side of the plasma is treated independently, and there is a difficulty in doing so in a self-consistent way. More precisely, one may create a “source sheath” at the vicinity of the boundary, which is clearly an undesirable effect (see for example [11]). For instance, a non-Maxwellian electron energy distribution function could get distorted if the potential drop across the source sheath  $\Delta\phi_{source}$  became comparable to the effective electron temperature  $T_{eff}$ . The present work addresses this problem, and a method is presented to deal with the particle loading and the electric field on the boundary. A source sheath is present but its magnitude is very small with a negligible effect on the simulation. The method has been successfully used for the study of collisionless heating by a capacitive rf sheath [12] and the simulation of a planar Langmuir probe [13]. Another solution to this problem in a magnetized system has been presented in [14].

The outline of the paper is as follows: In Section 2 we discuss briefly the implementation of the one ion species model. More details are given in Sections 2.1 and 2.2 concerning the boundary conditions, particle loading, and relaxation method. In Section 3, we provide the modifications needed to treat the multiple-ion case and finally, in Section 4, the special cases of collisionless and/or magnetized plasmas are considered and conclusions are drawn. The parameters chosen for the examples in this paper were taken to correspond to a capacitive discharge. Helium and argon model gases were used and a charge-exchange model was used for collisions assuming a constant collision frequency proportional to the pressure and the cross sections of each of the ions. The method however, does not depend on the collision handling and different schemes can be used trivially.

## 2. IMPLEMENTATION OF THE 1-ION SPECIES MODEL

Considering the case of a one ion-species isothermal plasma such that  $\nabla p = kT\nabla n$  and assuming that ionization is not an important process on the scales we are modeling (which is essentially equivalent to assuming that the simulation volume is small compared to the plasma volume), the common flux for both ions and electrons is equal to

$$\Gamma = -\frac{\mu_i D_e + \mu_e D_i}{\mu_i + \mu_e} \frac{dn}{dx} = -D_a \frac{dn}{dx}, \quad (1)$$

where  $\mu_s = |q_s|/m_s \nu_{ms}$  are the mobility coefficients,  $D_s = kT_s/m_s \nu_{ms}$  are the diffusion coefficient, and  $\nu_{ms}$  are the momentum transfer frequencies resulting from collisions of the relevant species.  $D_a$  is the ambipolar diffusion coefficient. The density profile of the species in the absence of ionization is linear in the bulk plasma and the electric field in the bulk is given by

$$E = \frac{D_i - D_e}{\mu_i + \mu_e} \frac{1}{n} \frac{dn}{dx}. \quad (2)$$

### 2.1. Boundary Conditions and Initial Loading

From the above discussion it is clear that the constant flux is the parameter that determines the behavior of the bulk plasma boundary. That is, having set a value for the flux and determining somehow what the density  $n_b$  should be at the boundary, one can solve for the

average velocity of the species at the boundary  $u_b = \Gamma/n_b$ . If in addition the gradient of the density is known at the boundary, the electric field at the boundary can be found by (2). We will discuss later in Section 2.2 how to obtain the values of the density and its gradient.

One way to determine the flux is to pick the density at the sheath edge as a control parameter for the simulation. Then, *assuming* that the ions will arrive at the sheath edge with an average velocity equal to the Bohm velocity  $u_B = (kT_e/m_i)^{1/2}$  [3], the flux of the ions is determined.

In order to start the simulation, we arbitrarily assume a linear density profile. Having the density  $n(x)$  at any point, we load ion super-particles obtained from a warm Maxwellian drifting at a velocity  $u(x)$  such that  $n(x)u(x) = \Gamma = \text{const}$ . Enough electron super-particles are loaded from a warm nondrifting Maxwellian to preserve quasi-neutrality. Different initial loading schemes could be implemented accounting for example for a density drop in the sheath region or for particles which have suffered collisions. These schemes will not be discussed here.

## 2.2. Particle Loading and Relaxation Method

The loading of the particles at the boundary has to be done from particle distributions, which are as consistent as possible with the desired physical boundary conditions. Failure to do so leads to the creation of an artificial “source sheath” at the boundary as for example in [11]. This happens mainly for two reasons:

- We inject in the simulation a drifted flux which essentially does not contain particles that have recently suffered collisions, whereas the “real” ion distribution at the boundary should contain a tail of low energy ions which have been affected by recent collisions. This effect will persist for a length of the order the ion mean free path, after which the ion distribution function will have relaxed (see Fig. 1).
- In the case when there is an *rf* component to the current drive, this should reflect on the electron fluxes that we load in the simulation. Therefore, in that case, the loading of electrons has to be done from drifting warm Maxwellian fluxes.

The procedure followed in a simulation step is illustrated in the flow chart in Fig. 2. Once the simulation is started, at every step  $\Gamma dt/\mathcal{W}_i$  ion super-particles are injected from the boundary in the simulation region, where  $\mathcal{W}_i$  is the number of real particles per super-particle. The particles are obtained from a warm drifting Maxwellian flux with drift velocity  $u_b$ , such that  $\Gamma = n_b u_b$ . Furthermore, assuming that  $\omega_{pe} \gg \omega \gg \omega_{pi}$ , all *rf* current is carried by the electrons while the displacement current is negligible, and the loading of the electrons is done in the following way: taking into account how much charge  $Q(t)$  has left or entered the simulation area from the bulk boundary (including the newly loaded ions) at that particular step, we inject enough electron super-particles as to conserve the total current (i.e.,  $(Q(t) - J_{DC}dt - J_{rf}dt)/e\mathcal{W}_e$  super-particles). The electron super-particles are picked from time-dependent warm drifting Maxwellian fluxes with a drift velocity equal to  $u_d(t) = J_{rf}(t)/en_b$ . In order to reduce the calculation time, the time-dependent fluxes are stored statically in an array.

As the simulation advances in time, we average the density profile in the proximity of the bulk boundary. At a certain time (usually several ion plasma periods), the average density profile near the bulk vicinity is fitted by a straight line. The extrapolation of the line to the boundary yields what the new density should be at the boundary, and again

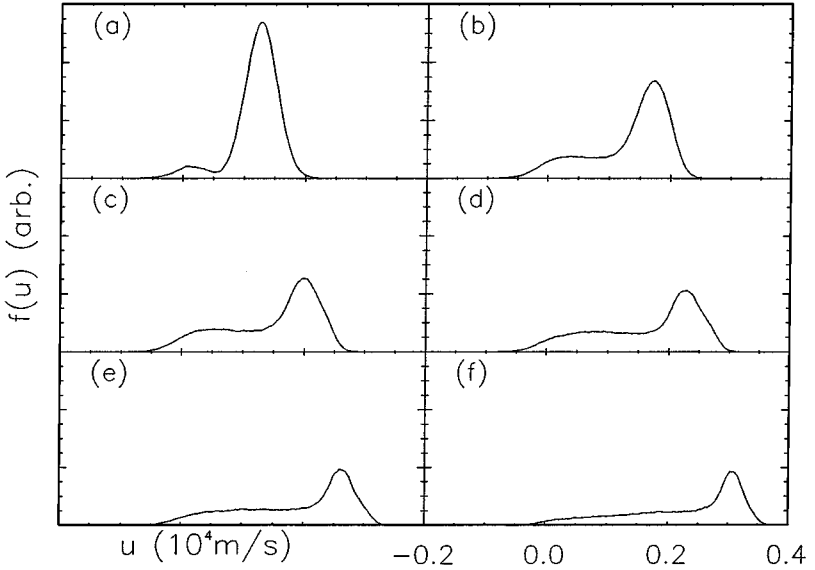


**FIG. 1.** The evolution in space of the ion velocity distribution function. At  $x = 0$ , the ion distribution function is composed by the super-position of the drifted Maxwellian that we inject and the ions that have been recently suffered collisions. Further toward the electrode, the ion velocity distribution function relaxes. The positions where the distributions were gathered were (a)  $x = 0.0$  cm, (b)  $x = 0.33$  cm, (c)  $x = 1.0$  cm and (d)  $x = 1.3$  cm and (e)  $x = 1.6$  cm. The potential drop across the source sheath was  $\Delta\phi_{source} = 0.04$  V. Conditions: Argon gas,  $I = 0$  A/m<sup>2</sup>,  $T_e = 2.57$  eV,  $T_i = 0.027$  eV,  $n_{sheath} \simeq 6.2510^{15}$  m<sup>-3</sup>,  $P = 10$  mTorr.

knowing the flux we alter the loading fluxes for both ions and electrons accordingly so as to account for the new drift velocities. Finally, the value of the electric field at the boundary is recalculated from (2). This process continues until steady state is reached. A typical result is shown in Fig. 3, where we plot the ion density. In that figure, a linear fit of the density in the bulk vicinity is also shown and the vertical line indicates the point at which the Bohm criterion is satisfied and quasi-neutrality breaks down. We can identify a bulk region (the region where the density drops linearly), a presheath region where the density profile departs from linearity and finally a sheath region. A small source sheath is also visible at the boundary.

### 3. IMPLEMENTATION OF THE MULTIPLE ION SPECIES MODEL

When more than one ion species is to be simulated, the complexity of the problem increases significantly and the analysis presented in Section 2 has to be modified. Specifically, there does not exist a common value for the ion and electron fluxes and therefore one cannot write equations similar to (1) and (2). In addition, although the electron density profile will still be linear (because of the higher mobility and diffusion coefficient of the electrons in comparison to any of the ions) the same does not necessarily happen to the ion density profiles. Finally, the hydrodynamic Bohm criterion in the case of multiple ion species [15] gives

$$\sum_i \frac{q_i^2 n_i}{m_i u_i^2} \geq \frac{e^2 n_e}{k T_e}, \quad (3)$$

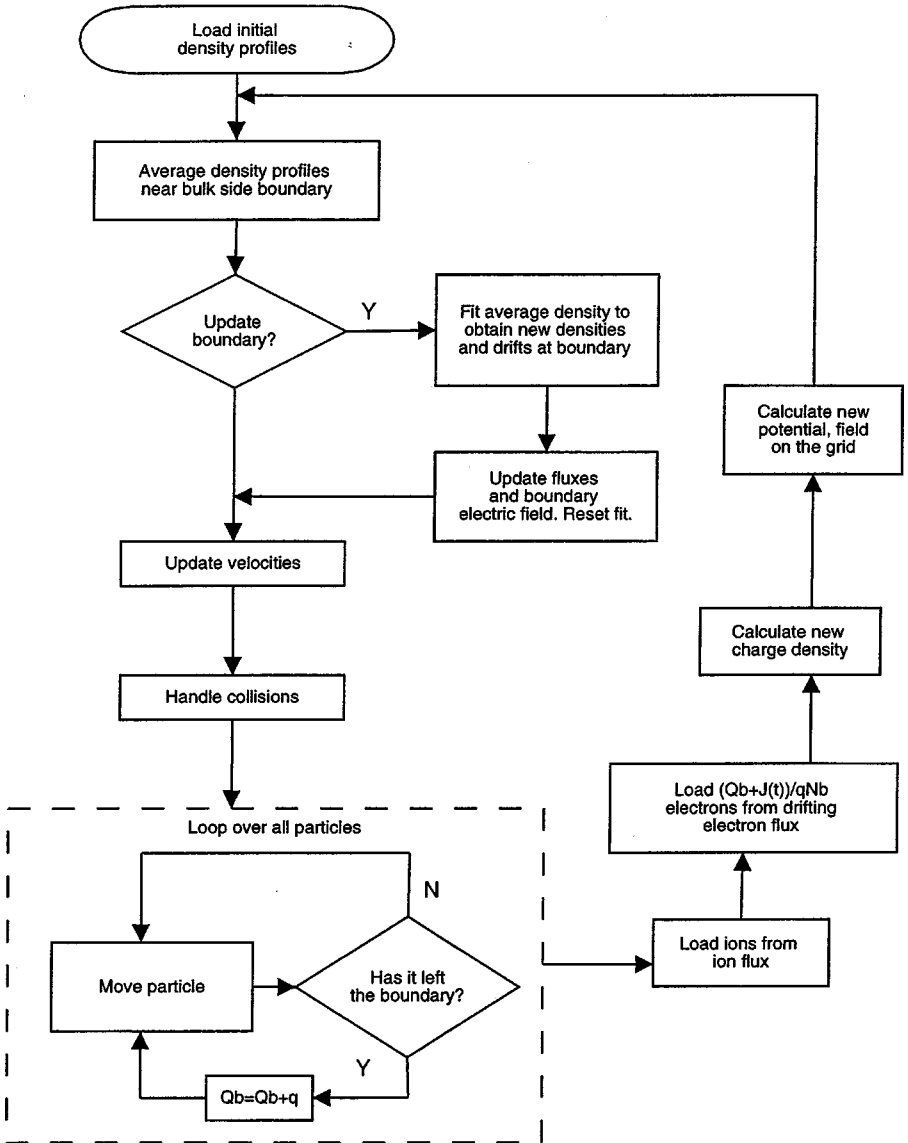
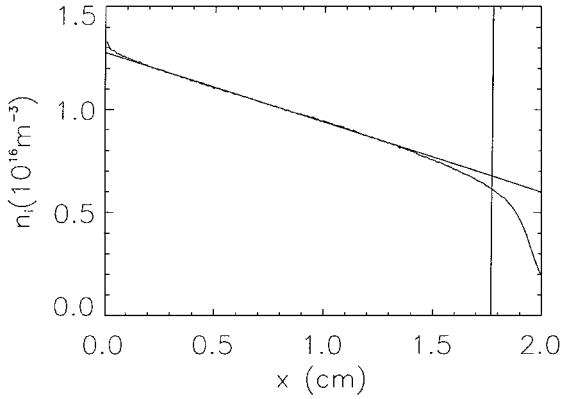


FIG. 2. Flow chart of the simulation procedure.

involving the individual densities of the ion species and therefore cannot be used directly to provide an estimate of the values of the individual ion fluxes. It is possible to overcome this problem by using extra equations to obtain closure. For instance, if only two ion species are considered, one can give an estimate of the floating potential, calculate the electron current, and then obtain one additional equation for the total ion flux from current conservation. This does not invalidate the method, as the simulation will still converge to a “real” solution of the problem for arbitrary ion fluxes, but the control that we had over the desired values of the densities at the sheath edge in the 1-ion case is lost. Once the individual ion fluxes are specified, the procedure we follow differs from the 1-ion case at the following points:



**FIG. 3.** The ion density profile. The solid curve corresponds to the ion density and the dashed line is a linear fit on the bulk part of the simulation region. The vertical line indicates the point where the Bohm criterion is satisfied and quasi-neutrality breaks (see text). The potential drop across the source sheath was  $\Delta\phi_{source} = 0.04$  V Conditions: Argon gas,  $I = 0\text{A/m}^2$ ,  $T_e = 2.57$  eV,  $T_i = 0.027$  eV,  $n_{sheath} \simeq 6.25 \cdot 10^{15}$   $\text{m}^3$ ,  $P = 10$  mTorr.

1. The densities of the ions at the boundary are all obtained from a second-order polynomial fit for each of the individual species. The electron density at the boundary is given by a linear fit.

2. As we noted already, the non self-consistent character of the fluxes that we inject at the boundary will always create a source-sheath. When more than one ion is used at low pressure the source-sheath becomes more significant because of interaction between the ion species. To deal with this, we sort the ion species by their collision frequency and perform the averaging for the electrons and all the ions except for the least collisional one. When the boundary is updated, the least collisional ion species takes its value not from a fit but using a quasi-neutrality condition.

3. The ambipolar electric field at the boundary is evaluated by fitting the potential at the bulk vicinity, instead of using the values of the calculated densities and density gradients.

An example of a simulation with two ions is shown in Fig. 4. Closer inspection reveals that as we mentioned already, the electron density is linear whereas the ion densities have a

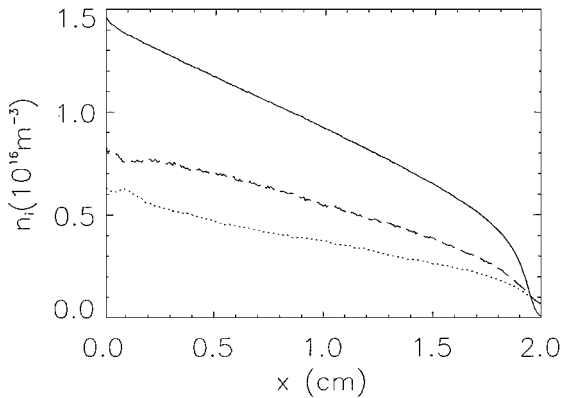


**FIG. 4.** Density profiles in the 2-ion case. The solid curve corresponds to the electron density and the dashed and dotted lines to the argon and helium densities, respectively. The potential drop across the source sheath was  $\Delta\phi_{source} = 0.03$  V Conditions:  $I = 0\text{A/m}^2$ ,  $T_e = 2.57$  eV,  $T_i = 0.027$  eV,  $n_{sheath} \simeq 2.01 \cdot 10^{15}$   $\text{m}^3$ ,  $P = 50$  mTorr.

slight curvature (one being concave and the other convex as to add up giving a linear profile in order to preserve quasineutrality). If the simulation size is increased, one of the ion density gradients goes to zero while the other ion's density gradient approaches the electron density gradient as we go far from the electrode.

#### 4. SPECIAL CASES

So far, we have dealt with plasmas that have some finite collision frequency. For some class of problems though, one would like to treat the plasma as completely collisionless. In that case, our analysis still applies but with some simplifications. The plasma structure is shown as obtained from our simulation in Fig. 5. It consists of a bulk plasma region where the density remains constant and a sheath region. A finite presheath region for the planar geometry cannot exist without collisions (in a cylindrical/spherical geometry, a geometrical presheath would be present). Therefore, the ions injected to the bulk region of the simulation have to already satisfy the Bohm criterion. The form of the IDF that is injected from the boundary is not particularly important since the sheath structure is not very sensitive to it. We have successfully tried Maxwellian distributions drifting at the Bohm velocity with various temperatures and Tonks–Langmuir distributions, without noticing significant differences. As far as the relaxation method is concerned, obviously it is not necessary in this case since the density at the boundary remains constant. This also makes the convergence faster.

Another possible use of the simulation scheme we propose is for the modeling of a plasma to which a constant magnetic field is applied. The method will still work in that case provided that the gyro-radius of the ions is large compared to the sheath dimensions. This could be used for instance for the modeling of the edges of fusion reactors.

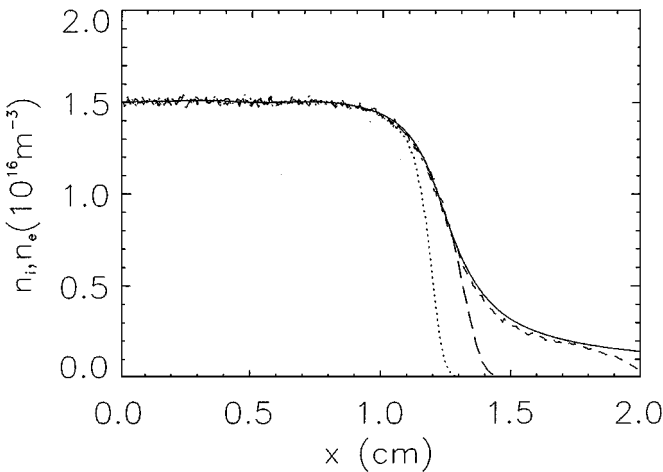


**FIG. 5.** Snapshots of the ion/electron density profile in the collisionless case. The solid line represents the average ion density and the short dashed, long dashed, and dotted lines the electron density at  $t = 0.0T_{rf}$ ,  $t = 0.25T_{rf}$ , and  $t = 0.5T_{rf}$ , respectively. The source sheath potential drop is not measurable. Conditions: Helium gas  $I_{rf} = 90 \text{ A/m}^2$ ,  $\omega_{rf}/2\pi = 13.56 \text{ MHz}$ ,  $T_e = 2.57 \text{ eV}$ ,  $T_i = 0.027 \text{ eV}$ .

## 5. CONCLUSIONS

We have presented a method that deals efficiently with the problems of boundary conditions and particle loading in semi-infinite PIC simulations. Our method applies to problems where ionization is not an important process in the scales assumed. The source sheath typically created in this type of simulations at the boundary is reduced in comparison with other simulations. This is done through self-consistent matching of the boundary and particle loading. The generalization of the process to deal with other geometries than planar is trivial, surface processes and constant magnetic fields can be included, and the completely collisionless plasma case can also be treated.

## ACKNOWLEDGMENT

This work is supported by Association EURATOM DCU Contract ERB 50004 CT960011.

## REFERENCES

1. V. A. Godyak and N. Sternberg, Dynamic model of the electrode sheaths in symmetrically driven rf discharges, *Phys. Rev. A*, **42**(4), 2299 (1990).
2. M. A. Lieberman, Analytical solution for capacitive rf sheath, *IEEE Trans. Plasma Sci.* **16**(6), 638 (1988).
3. K.-U. Riemann, The Bohm criterion and sheath formation, *J. Phys. D: Appl. Phys.* **24**, 518 (1991).
4. T. E. Nitschke and D. B. Graves, Matching an rf sheath model to a bulk plasma model, *IEEE Trans. Plasma Sci.* **23**(4), 717 (1995).
5. K.-U. Riemann, The influence of collisions on the plasma sheath transition, *Phys. Plasmas* **4**(11), 4158 (1997).
6. C. K. Birdsall and A. B. Langdon, *Plasma Physics via Computer Simulation* (Hilger, Bristol, 1991).
7. R. W. Hockney and J. W. Eastwood, *Computer Simulation Using Particles* (Hilger, Bristol, 1988).
8. C. K. Birdsall, Particle-in-cell charged-particle simulations, plus Monte Carlo collisions with neutral atoms, PIC-MCC, *IEEE Trans. Plasma Sci.* **19**(2), 65 (1991).
9. V. Vahedi, G. DiPeso, C. K. Birdsall, M. A. Lieberman, and T. D. Rognlien, Capacitive RF discharges modelled by particle-in-cell Monte Carlo simulation. I. analysis of numerical techniques, *Plasma Sources Sci. Technol.* **2**, 261 (1993).
10. V. Vahedi, C. K. Birdsall, M. A. Lieberman, G. DiPeso, and T. D. Rognlien, Capacitive RF discharges modelled by particle-in-cell Monte Carlo simulation. II. Comparison with laboratory measurements of electron energy distribution functions, *Plasma Sources Sci. Technol.* **2**, 273 (1993).
11. M. Surendra and D. Vender, Collisionless electron heating by radio-frequency plasma sheaths, *Appl. Phys. Lett.* **65**(2), 153 (1994).
12. G. Gozadinos, D. Vender, M. M. Turner, and M. A. Lieberman, Collisionless electron heating by capacitive radio-frequency plasma sheaths, *Plasma Sources Sci. Technol.* **10** (2001).
13. G. Gozadinos, D. Vender, and M. M. Turner, Self-consistent pic simulation of a planar probe, in *Proceedings of the XVth ESCAMPIG, Lillafured, Hungary*, 2000, pp. 318–319.
14. R. Chodura, Plasma-wall transition in an oblique magnetic field, *Phys. Fluids* **25**(9), 1628 (1982).
15. K.-U. Riemann, The Bohm Criterion and boundary conditions for a multicomponent system, *IEEE Trans. Plasma Sci.* **23**(4), 709 (1995).